

A Transcriptional Switch Mediated by Cofactor Methylation

Wei Xu,¹ Hongwu Chen,² Keyong Du,³ Hiroshi Asahara,³
 Marc Tini,¹ Beverly M. Emerson,⁴ Marc Montminy,³
 Ronald M. Evans^{1,5*}

We describe a molecular switch based on the controlled methylation of nucleosome and the transcriptional cofactors, the CREB-binding proteins (CBP)/p300. The CBP/p300 methylation site is localized to an arginine residue that is essential for stabilizing the structure of the KIX domain, which mediates CREB recruitment. Methylation of KIX by coactivator-associated arginine methyltransferase 1 (CARM1) blocks CREB activation by disabling the interaction between KIX and the kinase inducible domain (KID) of CREB. Thus, CARM1 functions as a corepressor in cyclic adenosine monophosphate signaling pathway via its methyltransferase activity while acting as a coactivator for nuclear hormones. These results provide strong *in vivo* and *in vitro* evidence that histone methylation plays a key role in hormone-induced gene activation and define cofactor methylation as a new regulatory mechanism in hormone signaling.

Steroids, retinoids, and thyroid hormones regulate expression of target genes through binding and activation of their corresponding nuclear receptors (NRs) (1). NRs are hormone-dependent transcription factors whose ligands promote the recruitment of coactivators and corepressors (2). Many NR coactivators have been identified, including three p160 family members, CBP/p300, the DRIP/TRAP/ARC complex, the RNA transcript SRA, as well as several chromatin remodeling factors (3). Among these, CBP/p300 participate in a variety of biological processes such as cellular differentiation, development, and growth control (4). CBP and p300 share highly conserved sequences including a bromodomain, a KIX domain, and three regions rich in Cys/His residues (C/H domains), which serve as docking sites for multiple transcription factors (5). CBP/p300 and p160 coactivators possess intrinsic histone acetyltransferase (HAT) activity, which is essential for transactivation in NR signaling (6).

The p160 coactivators (7, 8) associate with ligand-bound NRs directly and recruit other coactivators via two COOH-terminal activation domains, AD1 and AD2. AD1 recruits CBP/p300 whereas AD2 binds to coactivator-associated arginine methyltransferase 1 (CARM1), a protein methyltransferase (9). CARM1 methylates Arg², Arg¹⁷, and Arg²⁶ in the histone H3

NH₂-terminal tail (10). Studies by Chen *et al.* revealed a synergistic stimulation by p300 and CARM1 in the presence of GRIP1 in estrogen receptor activation function, suggesting that both the HAT activity of CBP/p300 and the histone methyltransferase activity (HMT) of CARM1 may cooperate in histone modification and thereby facilitate nucleosome remodeling and recruitment of transcriptional machinery (11). CARM1 belongs to the type I class of protein arginine methyltransferase (PRMT) (12). Recently, arginine methylation was reported to modulate protein-protein interaction (13, 14). However, no transcription factor has yet been demonstrated as a direct methylation target.

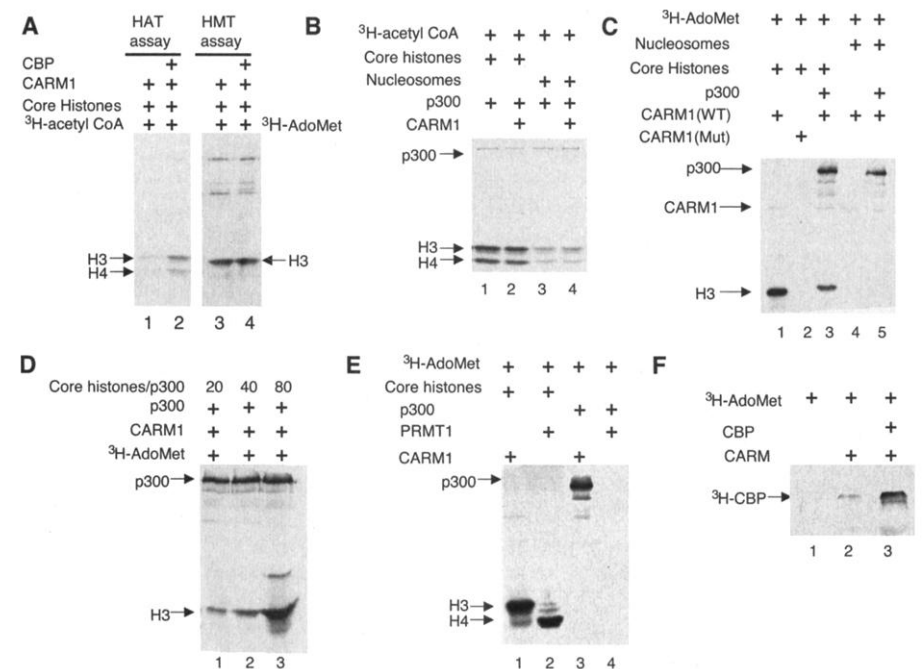
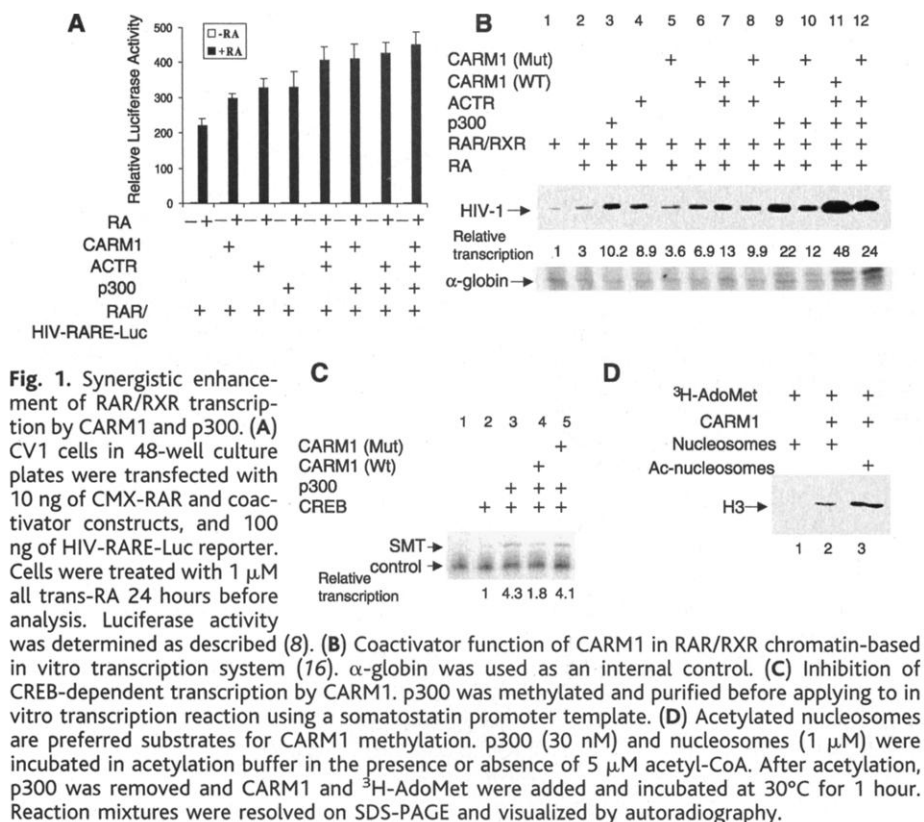
CARM1 enhances receptor-dependent transcription *in vitro*. In order to characterize the potential interplay between CARM1 HMT and p300 HAT in gene regulation, we initially performed transient transfection to examine the effect of CARM1 and p300 on RAR/RXR-dependent transcription. The p160-family cofactor ACTR (8) was included, because it interacts with both p300 and CARM1 through AD1 and AD2 motifs. As shown in Fig. 1A, various combinations of CARM1 (15) with p300 or ACTR produced modest but consistent enhancement of the reporter gene by RAR/RXR heterodimers. This result is consistent with previous observations made with several steroid receptors (11), although the presence of endogenous factors complicates the assay. To overcome this limitation, we employed recombinant factors in an *in vitro* chromatin-based RAR/RXR-dependent transcription system (15, 16). As shown in Fig. 1B, retinoic acid (RA) induced RARE-dependent transcription by 3.3-fold (lanes 1 and 2). ACTR and p300

further enhanced RA-dependent transcription by 8.9- and 10.2-fold, respectively (lanes 3 and 4). Whereas the combination of p300 and CARM1 synergistically enhanced transcription by 22-fold (lane 9), the combination of ACTR and CARM1 only slightly exceeded the effect of ACTR alone (13-fold, lane 7). The synergistic effect of CARM1 and p300 was observed (48-fold) when additional ACTR was added (lane 11), suggesting that a trimeric coactivator complex is required for maximal activation. The methyltransferase activity of CARM1 appeared to be essential, because a CARM1 mutant (¹⁸⁹VLD¹⁹¹ → AAA) defective in enzymatic activity exhibited no appreciable activation (lanes 5, 8, 10, and 12). Similarly, we analyzed the effect of CARM1 *in vitro* in a CREB-dependent transcription system. As shown in Fig. 1C, transcription on a CRE-template required phosphorylated CREB (lane 2). p300 enhanced transcription by 4.3-fold (lane 3). Wild-type CARM1 inhibited (lane 4), whereas mutant CARM1 exhibited no effect on (lane 5), p300 and CREB-dependent transcription. The opposing effect of CARM1 in nuclear receptor and CREB pathways is discussed later. To explore the possibility that methylation and acetylation of histones may cooperate in modifying chromatin structure, we compared CARM1 methylation on p300-acetylated versus nonacetylated nucleosomes (17). As shown in Fig. 1D, p300-acetylated nucleosomes were more effectively methylated (lane 3), whereas nonacetylated nucleosomes were poor substrates for CARM1 methylation (lane 2). The substrate preference for CARM1 methylation is in the order of free histones > acetylated nucleosomes > nonacetylated nucleosomes. These results indicate that CARM1 is a nuclear receptor cofactor through which methylation and acetylation might cooperate in modifying chromatin to stimulate transcription.

CBP/p300 are methylated by CARM1. In the supplemental figures (18), glutathione *S*-transferase (GST) pull-down, mammalian two-hybrid, and coimmunoprecipitation studies show that CARM1 and CBP/p300 interact directly both *in vivo* and *in vitro*. In addition, immunoprecipitation of CARM1 coprecipitates both HAT and HMT activities from 293T cell nuclear extracts (Fig. 2A). We then examined whether p300 HAT and CARM1 HMT activities were mutually regulated. In the *in vitro* acetylation assay (Fig. 2B), CARM1, which was not observably acetylated by p300, did not show any effect on the acetylation of histone (lanes 1 and 2) or nucleosome (lanes 3 and 4) by p300 *in vitro*. In the *in vitro* methylation assays (Fig. 2C), we analyzed the effect of p300 on CARM1 HMT. Wild-type CARM1, but not an HMT-defective mutant, methylated H3 in core histones (lanes 1 and 2). We found that, in addition to histones, p300 was strongly meth-

¹Gene Expression Laboratory, ²Department of Biological Chemistry, University of California Davis Cancer Center/Basic Science, Sacramento, CA 95817, USA. ³Peptide Biology Laboratory, ⁴Regulatory Biology Laboratory, The Salk Institute for Biological Studies, La Jolla, CA 92037, USA. ⁵Howard Hughes Medical Institute, La Jolla, CA 92037, USA.

*To whom correspondence should be addressed. E-mail: evans@salk.edu



ylated (lane 3). In the presence of nucleosomes, p300 was the preferred substrate (lanes 4 and 5). To examine this observation, a competition experiment was performed using increasing amounts of H3 to compete for p300 methylation. Even at a molar ratio of 80:1, the level of p300 methylation was not reduced (Fig. 2D, lanes 1 to 3). Thus, p300 is an efficient and not readily competed substrate for CARM1 methylation. Because p300 used in the reaction is approximately 30 nM and methylation of p300 appeared to be saturated, we reasoned that the K_m (affinity constant) for p300 is lower than 30 nM. This estimation is in conformity with the report that CARM1 exhibits an apparent K_m for H3 of 0.2 μ M (10). However, it is also highly probable that the preference for CBP is in part a consequence of the direct physical interaction which could create pseudo-first order kinetics.

We next compared the substrate specificities of CARM1 and p300 using other proteins including p53, PCAF, ACTR, and RAR/RXR. Although p53 is acetylated by p300, it is not methylated by CARM1. In contrast, ACTR is a substrate for both activities whereas neither RAR/RXR nor PCAF was a CARM1 substrate. It should be noted that p300 could be autoacetylated and CARM1 could be automethylated. To verify that p300 methylation is CARM1-specific, the related PRMT1 (19) was used as a comparison. PRMT1 is also a class I arginine methyltransferase that has recently been shown to methylate STAT1 (14). Though PRMT1 substantially methylated histone H4 (lane 2), methylation of p300 by PRMT1 was not detected (lane 4) (Fig. 2E). To demonstrate that p300/CBP is indeed arginine-methylated in vivo, we subjected cell lysates derived from δ -adenosyl- 3 H-methylmethionine (3 H-S-adoMet)-labeled cells to immunoprecipitation by antibody to CBP (anti-CBP) (20). Endogenous methylated CBP was detected in CARM1-transfected cells (Fig. 2F, lanes 1 and 2), although methylation was increased when CBP was cotransfected (lane 3). These results indicate that CBP/p300 can be a substrate for CARM1 methylation both in vitro and in vivo.

CARM1 inhibits KIX-KID interaction and CREB-dependent transcription. We examined the possibility that CBP/p300 methylation by CARM1 blocks the interaction between CBP/p300 (the KIX domain) and CREB (the KID domain). Results from a mammalian two-hybrid assay (Fig. 3A) showed that CARM1 attenuated the forskolin (FSK)-dependent KID-KIX interaction in a dose-dependent manner. Consistently, the nonmethylated KIX-containing p300 fragment efficiently supershifted with phospho-CREB (Fig. 3B, lane 6) in an electrophoretic mobility-shift assay (EMSA) (21), whereas the supershift was significantly impaired upon methylation (lane 5). Because CREB-dependent transcription is determined by the strength of the KID-KIX complex (22), we

hypothesized that CBP/p300 methylation could disrupt the interaction and result in an inhibition of CREB signaling. We examined the effect of CARM1 on the expression of a CREB target gene, somatostatin (SMT) that is previously known to be regulated by cyclic adenosine monophosphate (cAMP) (23). Whereas transfection of wild-type CARM1 blocked somatostatin expression in a dose-dependent manner, mutant CARM1 exhibited only a marginal effect (Fig. 3C). It has been reported that c-myc resembles CREB in binding to CBP (24); therefore, we analyzed whether transactivation by c-myc was also inhibited by CARM1. Again, we observed that wild-type, but not mutant CARM1, blocked GAL-myb activation in a dose-dependent manner (Fig. 3D). Thus, the CBP/p300 KIX region might be the methylation target.

CARM1 inhibits physiological function of CREB. The SMT gene contains a cAMP response element and is regulated by CREB and CBP/p300 (25). Therefore, we studied SMT gene expression after transfecting wild-type or HMT-defective CARM1 into a stably transfected somatostatin reporter cell line (26). Treatment of cells with FSK for 3 hours led to threefold induction of SMT expression (Fig. 4A, compare lane 2 with lane 1), indicating that SMT expression is cAMP-dependent. CARM1 resulted in a 50% reduction in SMT expression (lane 3), whereas mutant CARM1 has no inhibitory effect (lane 4). This result implied that the methyltransferase activity of CARM1 could inhibit SMT gene expression *in vivo*.

Neonatal sympathetic neurons are completely dependent on nerve growth factor (NGF), a member of the neurotrophin family of growth factors, for survival and differentiation (27). NGF promotes survival of neurons through activation of CREB and CREB-dependent expression of Bcl-2 in neuronal cells, such as PC12 (27). Therefore, inhibition of CREB signaling by CARM1 should enhance apoptosis. To test this hypothesis, we determined the effect of CARM1 on CREB- and NGF-induced cell survival in PC12 cells. Figure 4B shows a DNA fragmentation assay with CARM1-transfected and NGF-maintained cells. Wild-type CARM1 (lane 2) induced apoptosis, as indicated by the ladder of fragmented DNA, a hallmark of apoptosis (lane 5). This apoptotic effect was relieved when VP16-CREB was cotransfected (lane 4), supporting the idea that CARM1 acts by blocking CBP and CREB association, since VP16-CREB could bypass CARM1 inhibition. Transfection of mutant CARM1 resulted in only minor apoptosis (lane 3), implying that HMT activity is essential for the inhibition. To investigate whether the apoptotic effect of CARM1 is mediated through inhibition of Bcl2, we generated a CARM1-stable PC12 cell line (28) and examined its

effects on the NGF response. CARM1 cells, like wild-type cells, differentiate in response to NGF; however, they become apoptotic within 2 days. As determined by reverse transcription polymerase chain reaction (RT-PCR), expres-

sion of Bcl2 in CARM1 cells (Fig. 4C, lanes 2 and 4) was lower than that in PC12 cells (lanes 1 and 3) treated with the same dose of NGF. This result implies that CARM1-induced apoptosis is linked to the inhibition of Bcl2 induc-

Fig. 3. Methylation of CBP KIX domain inhibits CREB-dependent pathways. (A) Interaction between CREB KID and CBP KIX domains were analyzed by mammalian two-hybrid assay. MH100-TK-Luc reporter (35 ng), and Gal4-DBD-KID and VP16-KIX (15 ng each) were cotransfected with CMX-CARM1 in 293T cells. The next day, cells were treated with 10 μ M forskolin for 4 hours before collection. (B) Interaction of phosphorylated CREB with methylated or nonmethylated GST-p300 (301 to 800). (C) FSK-dependent somatostatin gene expression was inhibited by CARM1. We cotransfected 15 ng of somatostatin luciferase reporter and CMX-CARM1 constructs into 293T cells. Relative luciferase activities in the absence (white bar) and presence (black bar) of 10 μ M FSK are presented. (D) Gal-myb reporter gene expression was inhibited by CARM1.

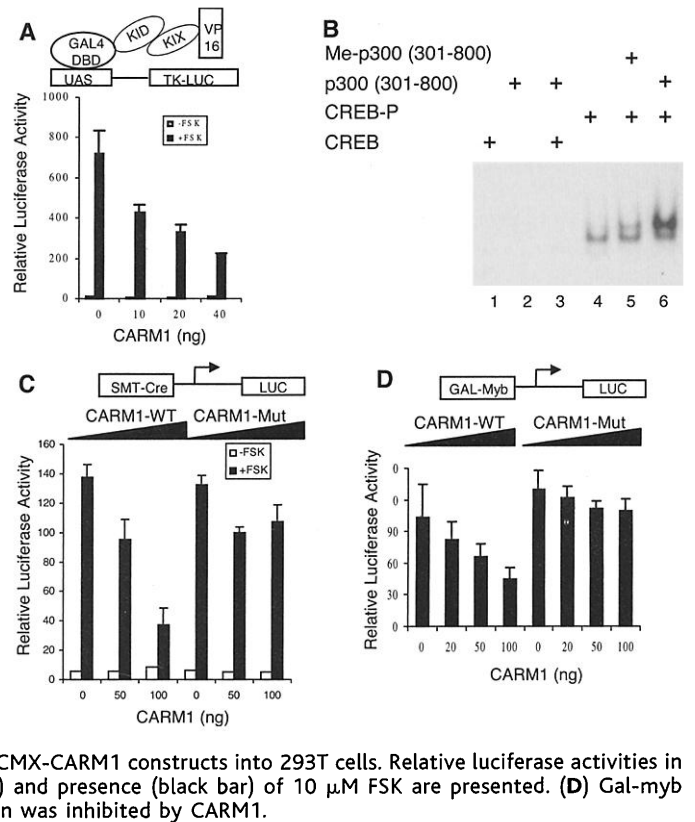
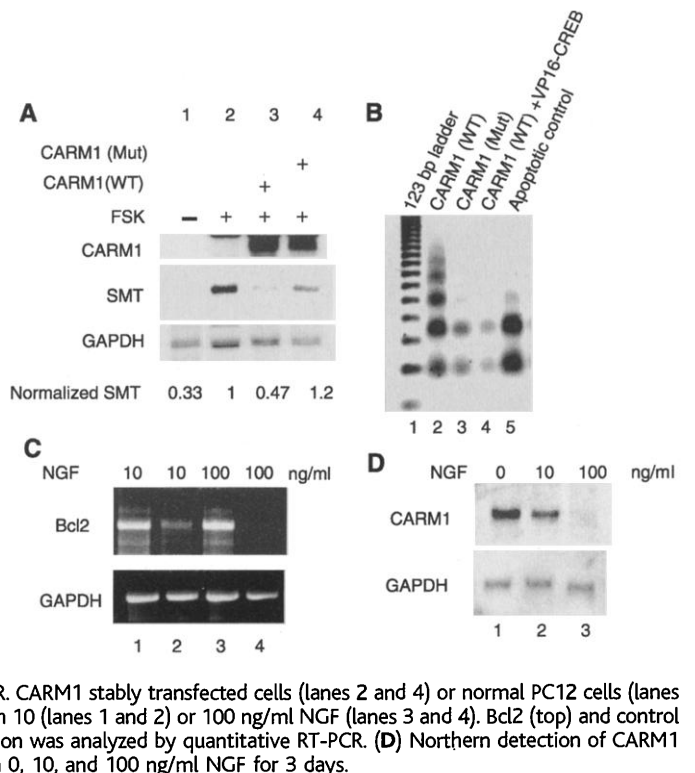


Fig. 4. CARM1 blocks the physiological function of CREB. (A) Endogenous somatostatin expression was inhibited by CARM1 methyltransferase activity. CMV-GFP (4 μ g) and mock vector (20 μ g) (lanes 1 and 2) or 20 μ g of wild-type (lane 3) or mutant CMX-CARM1 (lane 4) were cotransfected into NIH3T3 somatostatin-expressing stable cells. Cells (except in lane 1) were treated with forskolin 3 hours before sorting. GFP-transfected cells were used for RNA preparation. Relative levels of SMT RNA after normalization with GAPDH were indicated. (B) DNA fragmentation assay (18). (C) Analysis of Bcl2 expression by RT-PCR. CARM1 stably transfected cells (lanes 2 and 4) or normal PC12 cells (lanes 1 and 3) were treated with 10 (lanes 1 and 2) or 100 ng/ml NGF (lanes 3 and 4). Bcl2 (top) and control GAPDH (bottom) expression was analyzed by quantitative RT-PCR. (D) Northern detection of CARM1 in PC12 cells treated with 0, 10, and 100 ng/ml NGF for 3 days.



tion. A physiologic role for endogenous CARM1 was substantiated by the observation that its expression was dramatically decreased in NGF-treated cells (Fig. 4D). Accordingly, we conclude that CARM1-mediated CBP/p300 methylation disrupts CREB binding, and as a consequence, activates an apoptotic response.

Methylation of CBP KIX domain. To narrow the methylation region in CBP/p300, we employed *in vitro* methylation assays with GST fusion proteins encompassing the majority of sequence of p300 (29). Figure 5A shows that at least two fragments of p300 at the NH₂-terminus were methylated by CARM1. One of them, p300 (residues 1 to 300), contains a GRGR consensus methylation sequence by other PRMT family members (30), but was only weakly methylated (lane 1). The other, p300 (residues 301 to 800), which contains the KIX but has no apparent consensus sequence, was strongly methylated (lane 2). These results were confirmed with two CBP fragments (lanes 5 and 6) that include the KIX region. Further experiments showed that the KIX domain (residues 582 to 672) of CBP is the minimal region for methylation (31). Because the KIX domain contains a total of seven conserved arginines (Fig. 5B), we investigated the methylation of GST-KIX fusion proteins containing every single or double mutation in the arginine residues. As seen in Fig. 5C (upper panel), the R580K single-site mutation and the R648/649K double-site mutation both led to prominent reduction in the overall methyl-

ation. However, the R648/649K mutant protein was less stable (Fig. 5C, lower panel). We then analyzed the methylation of four synthetic peptides encompassing all the arginines in the KIX domain. Indeed, the peptide-covering R580 was methylated most efficiently by CARM1 in the filter-binding assay (Fig. 5D, left panel). Microsequencing of the peptides revealed that R580 is the most highly methylated, with R604 standing as the only other prominent modified residue in the KIX domain (Fig. 5D, right panel). In the CBP KIX and CREB KID NMR structure (32), R600 in CBP KIX, which is equivalent to R580 in p300, localized to the external surface of the KIX-KID complex. A critical interaction is observed between the aromatic residue Tyr⁶⁴⁰ and the positively charged Arg⁶⁰⁰, which constitutes the only interaction between helix 1 and 2 in the KIX domain (Fig. 5E). The importance of R600 is clear because mutation at this residue was found to destabilizing the complex (33), presumably due to the disruption of KIX overall structure. It appears therefore that single-site methylation plays a key role in determining the partitioning of CBP/p300 in different pathways.

Discussion. Histone acetylation and methylation have drawn growing attention in regulating gene transcription via chromatin modification. Of particular interest is the potential interplay between acetylase and methylase in maintaining dynamic balance of gene activation and silencing. Our evidence that

the H3 acetylated nucleosomes are preferentially methylated by CARM1 suggests there are rules to control chromatin modification, supporting the idea of an acetylation and possibly a methylation “code” as described by Allis (34). Each methylase may have its own “code” because acetylation of H4 by p300 inhibits its methylation by PRMT1 (35). Perhaps the most important extension of this “code” is the discovery that CBP/p300 itself is a methylation substrate. Whereas targeted phosphorylation of CBP/p300 occurs in the COOH-terminal half and enhances its HAT activity (36), methylated residues reside in the NH₂-terminal region and modulate CBP function without affecting HAT activity. Typically, NGF induces phosphorylation and activation of CBP/p300 in PC12 cells, whereas methylation antagonizes this process.

The advantage of methylation-directed cofactor switching is that it provides a simple yet effective form of cross-talk between two potentially competing signaling pathways [Web fig. 3 (18)]. When recruited to the NR complexes by p160 coactivators, CARM1 enhances transcription by methylating histones subsequent to histone acetylation. It has previously been shown that the critical domains on CBP/p300 for NR activation include the HAT-, bromo-, and p160-binding domains (37). The virtue of regulation through the KIX domain is that this region is not essential for NR function. Consistently, KIX methylation exhibits no apparent effect on NR-mediated transcription either *in vivo* or *in vitro*. Similarly, a p300 R580K mutant, which cannot be methylated at the key R580 residue, displays the same transcriptional activity as wild-type p300 (31). Thus, CARM1 is a direct positive activator for NRs, but an indirect modulator by inhibition of CREB-dependent pathways. Because multiple transcription factors bind this conserved domain, methylation at KIX may manifest broader effects by modulating several regulatory pathways.

In summary, this study reveals that CARM1 has both chromatin and nonchromatin substrates and that methylation can function as a unique transcriptional switch. In the context of our discovery, the methylation of CBP/p300 selectively impairs cAMP-induced transcription while stimulating nuclear receptor target genes. Because CBP/p300 and CREB-dependent signaling pathways are developmentally and physiologically important, CARM1 methylation might have unexpected broad biological significance.

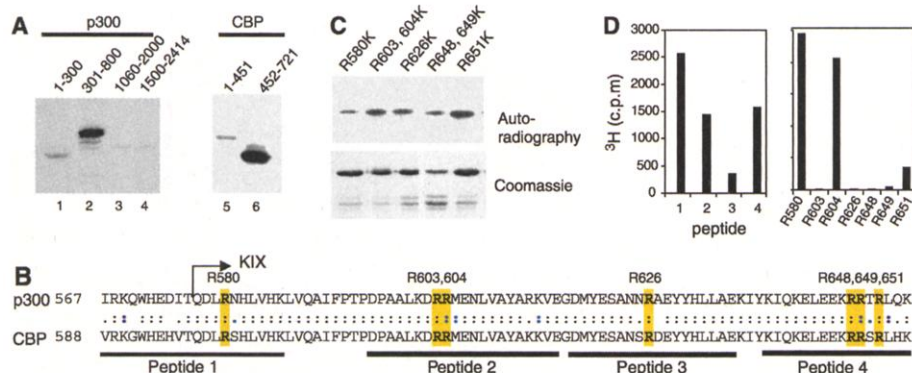
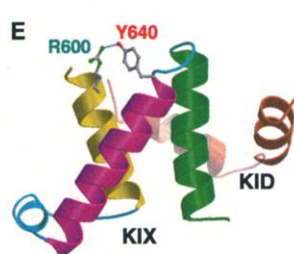


Fig. 5. p300/CBP is methylated at the KIX domain. (A) *In vitro* methylation of GST-p300 and GST-CBP fragments by CARM1. (B) Schematic representation of seven arginines in the p300 KIX domain (39). (C) Mutational analysis of p300 KIX domain arginines in the involvement of methylation by CARM1. (D) Identification of methylated arginines in the KIX domain. Total amounts of radioactivity associated with each peptide in the *in vitro* methylation and filter-binding assays (38) are shown (left). Peptides were microsequenced. Relative amounts of radioactivity on each R are indicated (right). (E) R600 in CBP KIX stabilizes the overall helix structure of CBP in the KIX-KID NMR structure. The three helical structures in CBP KIX are indicated with yellow, magenta, and green, respectively. The KID domain of CREB that interacted with KIX is shown in pink. Arginine 600 (green) and tyrosine 640 (red) in CBP form a unique hydrogen bond between helices 1 (yellow) and 2 (magenta). This model represents the average of 16 structures deposited in the Protein Data Bank (32).



References and Notes

1. N. J. McKenna, B. W. O'Malley, *J. Steroid Biochem. Mol. Biol.* **74**, 351 (2000).
2. L. Xu, C. K. Glass, M. G. Rosenfeld, *Curr. Opin. Genet. Dev.* **9**, 140 (1999).
3. B. D. Lemon, L. P. Freedman, *Curr. Opin. Genet. Dev.* **9**, 499 (1999).

4. R. H. Giles, D. J. Peters, M. H. Breuning, *Trends Genet.* **14**, 178 (1998).
5. R. H. Goodman, S. Smolik, *Genes Dev.* **14**, 1553 (2000).
6. I. J. McEwan, *Biochem. Soc. Trans.* **28**, 369 (2000).
7. J. Torchia et al., *Nature* **387**, 677 (1997); H. Hong, K. Kohli, A. Trivedi, D. L. Johnson, M. R. Stallcup, *Proc. Natl. Acad. Sci. U.S.A.* **93**, 4948 (1996); S. L. Anzick et al., *Science* **277**, 965 (1997); S. A. Oñate, S. Y. Tsai, M.-J. Tsai, B. W. O'Malley, *Science* **270**, 1354 (1995).
8. H. Chen et al., *Cell* **90**, 569 (1997).
9. D. Chen et al., *Science* **284**, 2174 (1999).
10. B. T. Schurter et al., *Biochemistry* **40**, 5747 (2001).
11. D. Chen, S. M. Huang, M. R. Stallcup, *J. Biol. Chem.* **275**, 40810 (2000).
12. J. M. Aletta, T. R. Cimato, M. J. Ettinger, *Trends Biochem. Sci.* **23**, 89 (1998).
13. M. T. Bedford et al., *J. Biol. Chem.* **275**, 16030 (2000).
14. K. A. Mowen et al., *Cell* **104**, 731 (2001).
15. The pSG5-CARM1 wild type and CARM1^{189VLD191} → AAA mutant were a kind gift from M. R. Stallcup. CARM1 cDNA was amplified with primers: 5' GGAATTCATATGGCAGCGCGGCAGCGACGG 3' and GAGCAGATCTCTAACTCCCATAGTGCATGGTGTGG 3' and subcloned into pFlag-AcSG2 (PharMingen). Recombinant CARM1 proteins were expressed in SF9 cells via the baculovirus system (PharMingen) and purified through Flag-M2 affinity resin. CARM1 cDNA was also subcloned into pCMX-L2 and pCMX-VP16 vectors to generate CMX-CARM1 and CMX-VP16-CARM1. Flag-tagged p300, ACTR, and PCAF were expressed and purified as described (8).
16. Chromatin was preassembled in Sf9 *Drosophila* extract for 4 hours at 27°C, then ~50 μM of each coactivator was added and the incubation extended for another 30 min. Transcription was initiated by addition of HeLa nuclear extract and dNTPs. Transcript amounts were analyzed by primer extension to determine the relative levels.
17. Acetylation and methylation assays were performed essentially as described (8, 9).
18. Supplemental material is available on Science Online at www.sciencemag.org/cgi/content/full/1065961/DC1
19. J. Tang et al., *J. Biol. Chem.* **275**, 7723 (2000).
20. Approximately 5 × 10⁶ 293T cells were transfected with CMX-CARM1 alone or with CMX-Flag CBP 1 day before the labeling. We added 50 μl of 486 μCi/ml S-AdoMet to 5 ml of methionine-depleted DMEM with dialyzed serum, and then applied to cells and incubated at 37°C for 4 hours. Immunoprecipitation with anti-CBP (A22, Santa Cruz) was performed as described (38).
21. Purified CREB proteins were in vitro phosphorylated by PKA (33). EMSA was performed as described (38).
22. A. J. Shaywitz, S. L. Dove, J. M. Kornhauser, A. Hochschild, M. E. Greenberg, *Mol. Cell. Biol.* **20**, 9409 (2000).
23. M. R. Montminy, K. A. Sevarino, J. A. Wagner, G. Mandel, R. H. Goodman, *Proc. Natl. Acad. Sci. U.S.A.* **83**, 6682 (1986).
24. D. Parker et al., *Mol. Cell. Biol.* **19**, 5601 (1999).
25. G. A. Gonzalez, M. R. Montminy, *Cell* **59**, 675 (1989).
26. M. R. Montminy et al., *J. Neurosci.* **6**, 1171 (1986).
27. A. Riccio, S. Ahn, C. M. Davenport, J. A. Blendy, D. D. Ginty, *Science* **286**, 2358 (1999).
28. CARM1 was subcloned into pLNCX (Clontech) between Hind III and Cla I sites. Phenix cells were transfected with pLNCX-CARM1 to produce retrovirus, which was then used for infection of PC12 cells. G418 (400 μg/ml) was used to select stably transfected cells. Expression of CARM1 was confirmed by Western blotting.
29. Portions of p300 (amino acids 1 to 300, 301 to 800, 1060 to 2000, and 1500 to 2414) were expressed as GST fusion proteins in *Escherichia coli* as described in D. Chakravarti et al. [*Nature* **383**, 99 (1996)].
30. S. Kim et al., *Biochemistry* **36**, 5185 (1997).
31. W. Xu et al., data not shown.
32. I. Radhakrishnan et al., *Cell* **91**, 741 (1997).
33. D. Parker et al., *Mol. Cell. Biol.* **16**, 694 (1996).
34. T. Jenuwein, C. D. Allis, *Science* **293**, 1074 (2001).
35. H. Wang et al., *Science* **293**, 853 (2001).
36. S. Ait-Si-Ali et al., *Biochem. Biophys. Res. Commun.*

- 262**, 157 (1999); N. D. Perkins et al., *Science* **275**, 523 (1997).
37. W. L. Kraus, J. T. Kadonaga, *Genes Dev.* **12**, 331 (1998).
38. H. Chen, R. J. Lin, W. Xie, D. Wilpitz, R. M. Evans, *Cell* **98**, 675 (1999).
39. Single-letter abbreviations for the amino acid residues are as follows: A, Ala; C, Cys; D, Asp; E, Glu; F, Phe; G, Gly; H, His; I, Ile; K, Lys; L, Leu; M, Met; N, Asn; P, Pro; Q, Gln; R, Arg; S, Ser; T, Thr; V, Val; W, Trp; and Y, Tyr.
40. We are grateful to C. Park and F. Wolfgang for the peptide analysis. We acknowledge M. Stallcup and H. R. Herschman for providing reagents. We thank Y. Ouyang, A. Lee, H. Juguilon, and J. Havstad for technical help, and L. Ong and E. Stevens for administrative assistance. We are grateful to R. Yu, R. Lin, W. Xie, T. Sternsdorf, C. Tsai for critical reading of the manuscript. R.M.E. is an investigator of the Howard Hughes Medical Institute at the Salk Institute and March of Dimes Chair in Molecular and Developmental Biology. Supported by a grant from the National Institute of Diabetes and Digestive and Kidney Diseases (9R01DK57978).

4 September 2001; accepted 12 October 2001
Published online 8 November 2001;
10.1126/science.1065961
Include this information when citing this paper.

Regulation of Daily Locomotor Activity and Sleep by Hypothalamic EGF Receptor Signaling

Achim Kramer,^{1*} Fu-Chia Yang,^{1†} Pamela Snodgrass,^{2‡} Xiaodong Li,^{2†} Thomas E. Scammell,³ Fred C. Davis,² Charles J. Weitz^{1‡}

The circadian clock in the suprachiasmatic nucleus (SCN) is thought to drive daily rhythms of behavior by secreting factors that act locally within the hypothalamus. In a systematic screen, we identified transforming growth factor- α (TGF- α) as a likely SCN inhibitor of locomotion. TGF- α is expressed rhythmically in the SCN, and when infused into the third ventricle it reversibly inhibited locomotor activity and disrupted circadian sleep-wake cycles. These actions are mediated by epidermal growth factor (EGF) receptors on neurons in the hypothalamic subparaventricular zone. Mice with a hypomorphic EGF receptor mutation exhibited excessive daytime locomotor activity and failed to suppress activity when exposed to light. These results implicate EGF receptor signaling in the daily control of locomotor activity, and identify a neural circuit in the hypothalamus that likely mediates the regulation of behavior both by the SCN and the retina.

Circadian rhythms of behavior in mammals are robust and precise. For example, in constant darkness and temperature, the circadian rhythm of locomotor activity in laboratory rodents persists indefinitely (1) and is accurate to within a few minutes per day (2, 3). The circadian clock driving locomotor activity and other circadian behaviors, such as the sleep-wake cycle, is located within the suprachiasmatic nucleus (SCN) of the hypothalamus (4).

The molecular mechanisms by which the SCN drives circadian rhythms of locomotor activity and other behaviors are unknown. In-

triguing clues, however, have come from SCN transplant studies. In animals made arrhythmic by SCN lesions, SCN grafts drive circadian rhythms of locomotor activity (5), even if the grafts are encapsulated (to prevent extension of axons but allow diffusion of secreted factors) (6). A study of "temporal chimeras" (7), hamsters with functional SCN tissue of both wild-type and short-period mutant genotypes, indicated that the SCN inhibits locomotor activity at one phase and promotes it at another, with inhibition dominating when the two influences coincided. These and related studies (8–10) suggest that the SCN drives circadian rhythms of locomotor activity by secreting at least one "locomotor inhibitory factor" at one phase and at least one "locomotor activating factor" at another. Although the effects of SCN grafts are mediated by factors secreted into the third ventricle of the hypothalamus in a paracrine fashion, it is possible in the intact animal that the secreted SCN factors act synaptically (6).

Transplant experiments indicate that the receptors for the secreted SCN factors are located

¹Department of Neurobiology, Harvard Medical School, Boston, MA 02115, USA. ²Department of Biology, Northeastern University, Boston, MA 02115, USA. ³Department of Neurology, Beth Israel Deaconess Medical Center and Harvard Medical School, Boston, MA 02115, USA.

*Present address: Institute for Medical Immunology, Humboldt University, 10098 Berlin, Germany.

†These authors contributed equally to this work.

‡To whom correspondence should be addressed. E-mail: cweitz@hms.harvard.edu